

## 3D QSAR Study on Pyrrolopyrimidines-Based Derivatives as LIM2 Kinase Inhibitors

Pavithra K. Balasubramanian<sup>1†</sup>, Anand Balupuri<sup>1†</sup>, and Seung Joo Cho<sup>1,2†</sup>

### Abstract

LIM kinases belong to the serine/Threonine kinase family. The members of the LIM kinase (LIMK) family include LIMK 1 and 2 which are involved in the regulation of actin polymerisation and microtubule disassembly. LIMK1 was shown to be involved in cancer metastasis, while LIMK2 activation promotes cells cycle progression. Since LIMK2 plays a vital role in many disease conditions such as pulmonary hypertension, cancer and viral diseases, and till date there are not much selective inhibitors been reported, LIMK2 becomes an interesting therapeutic target among the kinases. 3D QSAR study was carried out on a series of pyrrolopyrimidines based derivatives as LIMK2 inhibitors. A reasonable CoMFA ( $q^2=0.888$ ;  $ONC=3$ ;  $r^2=0.974$ ) with good statistical values was developed. The developed model was validated using 1000 runs of bootstrapping and was found to be predictable. The results of CoMFA contour map analysis suggested that the bulky substitution at R<sub>4</sub> and R<sub>5</sub> position are highly desirable to increase the activity. Similarly, positive substitution at R<sub>3</sub> position is also required to increase the activity. It is also noted that bulky substitution at R<sub>1</sub> position must be avoided. Our results could provide valuable information to enhance the activity of the LIMK2 inhibitors and to design potent pyrrolopyrimidines derivatives.

**Keywords:** LIMK2, CoMFA, Pyrrolopyrimidines, LIM Kinase, Inhibitors

### 1. Introduction

The LIM kinase (Lin-11/Isl-1/Mec-3 domain-containing protein kinase) is a serine/threonine kinase. LIM family consists of two members, LIM kinase 1 (LIMK1)<sup>[1]</sup> and LIM kinase 2 (LIMK2)<sup>[2]</sup>. LIMK1 and LIMK2 are closely-related proteins containing two N-terminal LIM domains, a PDZ domain and one C-terminal kinase domain. Both the LIM kinases have LIM domains and found to influence the architecture of the actin cytoskeleton by regulating the activity of the cofilin family proteins such as cofilin1, cofilin2 and destrin<sup>[3]</sup>. Both LIMK1 and LIMK2 are phosphorylated by small GTPases of Rho effector Rho kinase (ROCK) on conserved threonine residues, Thr- 508 in LIMK1 and Thr-505 in LIMK2<sup>[4-6]</sup>.

Like many other kinases, phosphorylation results in

increased LIMK activity. Recent works indicates that LIMK activity is also modulated by HIV-1 viral proteins. LIMK inhibitors have been believed to treat several conditions, including cancer, elevated intraocular pressure (IOP) and glaucoma, pulmonary hypertension and viral diseases<sup>[7-10]</sup>. It has also been identified that LIMK1 is activated by HIV-1 in order to initiate viral infection. ADF/cofilin are the only substrates identified for LIM kinases. In comparison with the other kinase targets, number of reported LIMK inhibitor series remains limited for LIM kinases.

The most potent LIMK inhibitors reported up-to date are based on pyrrolopyrimidines<sup>[6, 7]</sup> or 2-aminothiazole scaffolds<sup>[11]</sup>. LX-7101 (Lexicon Pharmaceuticals) was evaluated in a Phase-I trial as an IOP-lowering agent for treatment of glaucoma and it's the only LIMK inhibitor that reached clinical trials to date. This compound however shows inhibitory activity against ROCKs<sup>[8]</sup>. Hence, LIMK inhibitors of sufficient stability and selectivity must be identified. Our group has reported several research and review articles on various *insilico* techniques such as application of partial charges, molecular docking, and 3D-QSAR studies<sup>[12-16]</sup>. In this study, we

Departments of <sup>1</sup>Bio-New Drug Development and <sup>2</sup>Cellular/Molecular Medicine, College of Medicine, Chosun University, Gwangju 501-759, Korea

<sup>†</sup>Corresponding author : pavithrabioinfo@gmail.com, anandbalupuri.niper@gmail.com, chosj@chosun.ac.kr  
(Received: October 16, 2015, Revised: December 16, 2015  
Accepted: December 25, 2015)

have performed a CoMFA study on series of pyrrolopyrimidines based derivatives as LIMK2 inhibitors.

## 2. Methodology

### 2.1. Data Set

Data set of 27 pyrrolopyrimidines based derivatives used in this report were synthesized by Boland *et al.*,<sup>[17]</sup>. All the reported IC<sub>50</sub> values were converted into pIC<sub>50</sub>

values (-logIC<sub>50</sub>). SybylX2.1 was used to sketch all the dataset compounds<sup>[18]</sup>. The structure of the most active compound **27** was drawn and geometry of the molecule was optimized using sybyl Tripos force field. The energy optimized conformation of compound **27** was taken as the active conformation to draw the rest of the molecules in the dataset. The molecules taken for the study are shown in Table 1. Alignment of the dataset compounds was done using compound **27** as template molecule.

**Table 1.** Structure and Biological values of pyrrolopyrimidines based derivatives as LIM2 kinase inhibitors

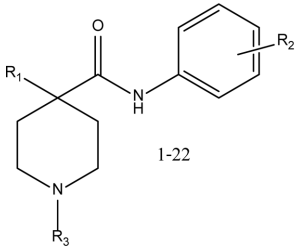
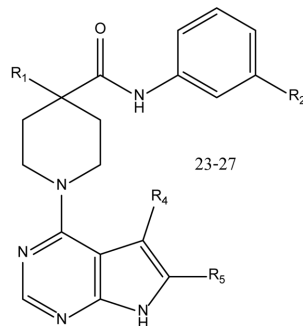
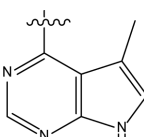
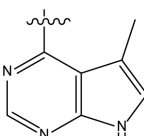
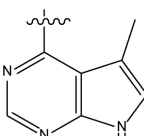
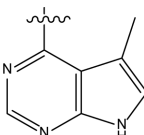
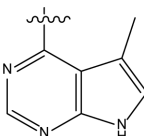
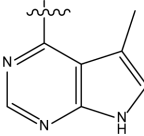
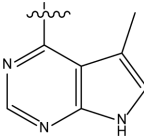
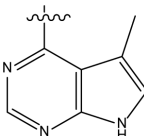
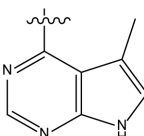
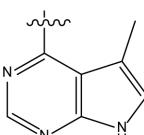
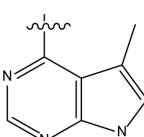
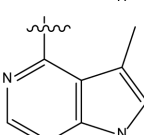
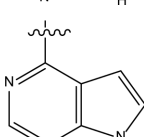
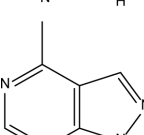
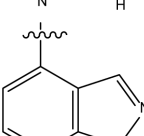
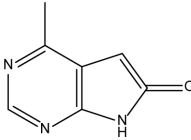
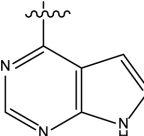
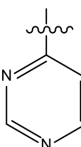
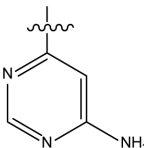
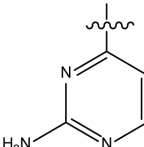
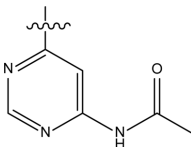
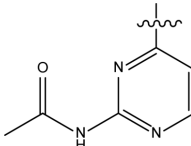
Compound	R <sub>1</sub>	R <sub>2</sub>	R <sub>3</sub>	R <sub>4</sub>	R <sub>5</sub>	pIC <sub>50</sub>
						
1	CH <sub>2</sub> NH <sub>2</sub>	3-CO <sub>2</sub> Me		-	-	9.000
2	CH <sub>2</sub> NMe <sub>2</sub>	3-OCONMe <sub>2</sub>		-	-	9.000
3	CH <sub>2</sub> NMe <sub>2</sub>	3-CO <sub>2</sub> Me		-	-	8.824
4	NH <sub>2</sub>	3-CO <sub>2</sub> Me		-	-	8.131
5	CH <sub>2</sub> NMe <sub>2</sub>	3-CO <sub>2</sub> Me		-	-	7.921

Table 1. Continued

Compound	R <sub>1</sub>	R <sub>2</sub>	R <sub>3</sub>	R <sub>4</sub>	R <sub>5</sub>	pIC <sub>50</sub>
6	NMe <sub>2</sub>	3-OCH <sub>2</sub> CO <sub>2</sub> Me		-	-	9.000
7	CH <sub>2</sub> NMe <sub>2</sub>	3-CH <sub>2</sub> CO <sub>2</sub> Me		-	-	9.000
8	CH <sub>2</sub> NMe <sub>2</sub>	4-CO <sub>2</sub> Me		-	-	8.114
9	CH <sub>2</sub> NMe <sub>2</sub>	3-CO <sub>2</sub> <i>n</i> -Pr		-	-	8.678
10	CH <sub>2</sub> NMe <sub>2</sub>	3-CO <sub>2</sub> <i>i</i> -Pr		-	-	8.658
11	CH <sub>2</sub> NMe <sub>2</sub>	3-CO <sub>2</sub> <i>sec</i> -Bu		-	-	8.337
12	CH <sub>2</sub> NMe <sub>2</sub>	3- CO <sub>2</sub> CH <sub>2</sub> CCH		-	-	9.000
13	CH <sub>2</sub> NMe <sub>2</sub>	3-CO <sub>2</sub> Me		-	-	7.886
14	CH <sub>2</sub> NMe <sub>2</sub>	3-CO <sub>2</sub> Me		-	-	6.714
15	CH <sub>2</sub> NMe <sub>2</sub>	3-CO <sub>2</sub> Me		-	-	6.562

**Table 1.** Continued

Compound	R <sub>1</sub>	R <sub>2</sub>	R <sub>3</sub>	R <sub>4</sub>	R <sub>5</sub>	pIC <sub>50</sub>
16	CH <sub>2</sub> NMe <sub>2</sub>	3-CO <sub>2</sub> Me		-	-	5.730
17	NH <sub>2</sub>	3-CO <sub>2</sub> Me		-	-	8.018
18	NH <sub>2</sub>	3-CO <sub>2</sub> Me		-	-	5.000
19	NH <sub>2</sub>	3-CO <sub>2</sub> Me		-	-	5.341
20	NH <sub>2</sub>	3-CO <sub>2</sub> Me		-	-	5.000
21	NH <sub>2</sub>	3-CO <sub>2</sub> Me		-	-	6.306
22	NH <sub>2</sub>	3-CO <sub>2</sub> Me		-	-	5.000
23	CH <sub>2</sub> NMe <sub>2</sub>	OCONMe <sub>2</sub>	-	CN	H	8.398
24	CH <sub>2</sub> NMe <sub>2</sub>	OCONMe <sub>2</sub>	-	F	H	8.553
25	CH <sub>2</sub> NMe <sub>2</sub>	OCONMe <sub>2</sub>	-	H	Me	8.097
26	CH <sub>2</sub> NMe <sub>2</sub>	OCONMe <sub>2</sub>	-	Me	Me	8.796
27	CH <sub>2</sub> NMe <sub>2</sub>	OCONMe <sub>2</sub>	-	Me	Me	8.854

## 2.2. CoMFA

CoMFA was developed by Cramer *et al*<sup>[19]</sup>. In the generation of CoMFA models, the aligned molecules were placed in a 3D cubic lattice box (2-Å grid spacing). Electrostatic and steric fields in CoMFA were calculated from Coulomb and Lennard-Jones potentials,

respectively. CoMFA steric and electrostatic fields were calculated by using probe atom (Csp<sup>3</sup>+1). The computed field energies with the standard cutoffs of 30 kcal/mol were used as independent variables. Different partial charges were applied to generate various CoMFA models. Out of these, a model with best statistical val-

ues in terms of  $q^2$ ,  $r^2$  and SEE was selected as the final model.

A leave-one-out (LOO) PLS was performed to determine the cross-validated  $r^2$  ( $q^2$ ) and the optimum number of components and minimum standard error of prediction (SEP) in the model. CoMFA descriptors were used as independent variables and  $\text{pIC}_{50}$  values were used as dependent variables in the PLS analysis. The cross-validated correlation coefficient ( $q^2$ ) that was obtained was considered for further analysis. The non-cross-validated analysis was performed to determine conventional Pearson correlation coefficient ( $r^2$ ), standard error of estimate (SEE) and Fischer's ratio (F) using the ONC previously obtained from the cross-validation method. All the developed models were validated to check its predictability using 1000 runs of bootstrapping.

### 3. Results and Discussion

#### 3.1. CoMFA Model

Various CoMFA models were developed for a series of pyrrolopyrimidines based derivatives using different partial charge schemes. Lowest energy conformer of the most active compound **27** was considered as template. All the molecules were then aligned over the template using alignment method based on the common substructure. The common substructure of the compounds from template molecule **27** is shown in Fig. 1 and the alignments of the compounds are displayed in Fig. 2. CoMFA models based on different partial charges were developed (Table 2). A reliable CoMFA model with good statistical values for the complete set of dataset compounds was obtained ( $q^2=0.888$ ,  $\text{NOC}=3$ ,  $r^2=0.974$ ) with Pullman charges as partial charge. The model was

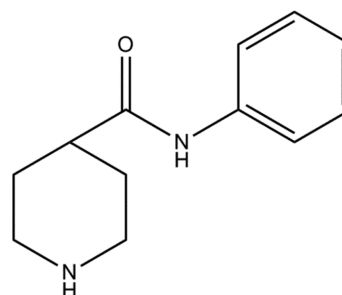


Fig. 1. Common Substructure from template compound **27**.

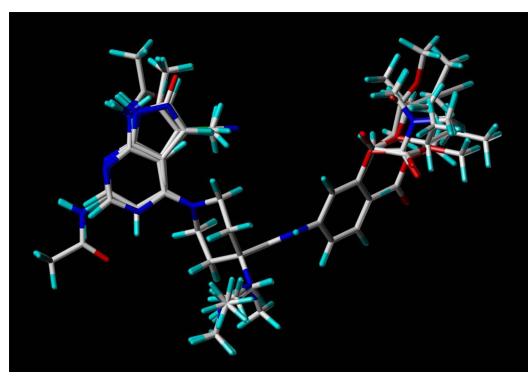


Fig. 2. Alignment of all the molecules used for CoMFA.

found to be reliable in terms of  $q^2$  and  $r^2$  values. Given that the total number of compounds are less than 30, the data set was not divided into training and test set. The bootstrapping  $r^2$  mean (BS- $r^2$ ) and BS- standard deviation (BS-SD) was 0.979 and 0.009 respectively. The model exhibited overall satisfactory statistical values. The detailed statistical values for the final selected CoMFA model are shown in Table 3. The experimental and predicted activity values of the molecules obtained

Table 2. Statistical summary of the developed CoMFA models with different charge schemes

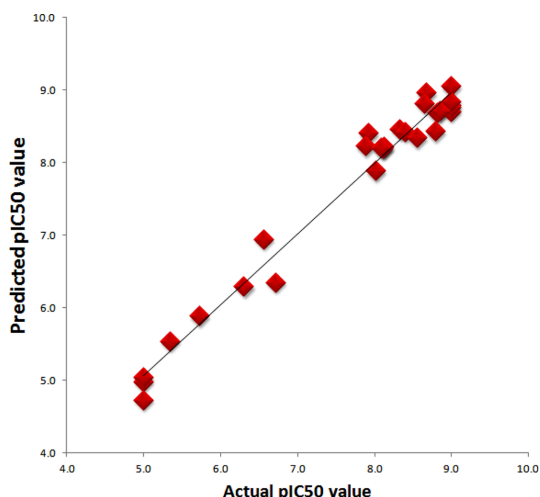
Parameter	Gasteiger-Huckel	Gasteiger-Marsili	Formal charges	MMFF94	Del-re	Huckel	Pullman
$q^2$	0.877	0.848	0.841	0.863	0.780	0.854	<b>0.888</b>
N	4	3	3	3	5	3	<b>3</b>
SEP	0.539	0.586	0.600	0.557	0.738	0.574	<b>0.502</b>
$r^2$	0.979	0.959	0.931	0.964	0.986	0.988	<b>0.974</b>
SEE	0.222	0.306	0.396	0.205	0.191	0.179	<b>0.243</b>
F	257.168	117.107	102.780	205.236	232.878	265.799	<b>285.653</b>

$q^2$  = cross-validated correlation coefficient; N = number of components; SEP = standard error of prediction;  $r^2$  = correlation coefficient; SEE = standard error of estimate; F = F-ratio.

**Table 3.** Detailed statistical summary of the selected CoMFA model

Parameters	CoMFA MODEL
$q^2$	0.888
NOC	3
SEP	0.502
$r^2$	0.974
SEE	0.243
F value	285.653
BS $r^2$	0.979
BS SD	0.009
Steric contribution	44.9
Electrostatic contribution	55.1

$q^2$ : cross-validated correlation coefficient; NOC: Number of components; SEP: Standard Error of prediction;  $r^2$ : non-validated correlation coefficient; SEE: Standard Error of Estimation; F value: F-test value; BS- $r^2$ : Bootstrapping  $r^2$  mean; BS-SD: Bootstrapping Standard deviation.

**Fig. 3.** Scatter plot diagram for final CoMFA model.

for the final CoMFA model is tabulated in Table 4. The scatter plot and contour map for the same are shown in Fig. 3 and Fig. 4 respectively.

### 3.2. CoMFA Contour Maps

The 3D contour plots graphically interpreting the CoMFA models were generated using the standard STDEV\*COEFF field type with the default 80% and 20% level contributions for favorable and unfavorable regions, respectively. The most active compound **27** was shown superimposed inside the contour map. The

**Table 4.** Actual and predicted  $pIC_{50}$  with their residuals of the developed CoMFA model

Compound	Actual $pIC_{50}$	CoMFA	
		Predicted	Residual
1	9.000	8.793	0.207
2	9.000	8.707	0.293
3	8.824	8.692	0.131
4	8.131	8.219	-0.089
5	7.921	8.404	-0.483
6	9.000	9.056	-0.056
7	9.000	8.759	0.241
8	8.114	8.193	-0.079
9	8.678	8.964	-0.286
10	8.658	8.816	-0.158
11	8.337	8.462	-0.125
12	9.000	8.846	0.154
13	7.886	8.228	-0.342
14	6.714	6.350	0.364
15	6.562	6.946	-0.384
16	5.730	5.888	-0.158
17	8.018	7.887	0.131
18	5.000	4.984	0.016
19	5.341	5.539	-0.198
20	5.000	4.729	0.271
21	6.306	6.289	0.017
22	5.000	5.039	-0.039
23	8.398	8.429	-0.031
24	8.553	8.341	0.212
25	8.097	8.204	-0.107
26	8.796	8.439	0.357
27	8.854	8.714	0.140

steric contour map of the selected CoMFA model is shown in Fig. 4a. The green color signifies regions that favor sterically bulky groups and yellow color signifies the regions that are not favored for bulky substitution. A green colour contour near the  $R_4$  and  $R_5$  position suggest that the bulky substitution that region could aid in the increased activity. This might be the reason for the high activity of compound **26** and the most active compound **27** which possess bulky substitution in that position. Similarly compounds **3**, **23**, **24** and **25** which contains bulky substituent in one of these positions ( $R_4$  or  $R_5$ ) show better activity compared to the rest of the dataset compounds. It is also observed that compounds **18**, **20**, and **22** which don't possess any substitution at

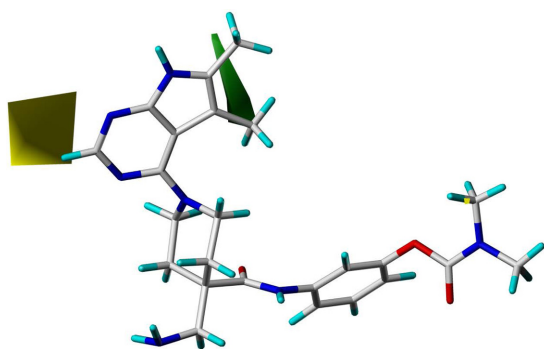


**Fig. 4a.** CoMFA Steric contour map. The green contours indicate sterically favored regions and the yellow contours denote the sterically unfavorable regions.

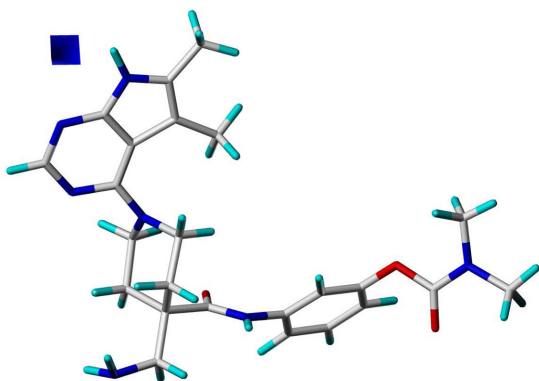


**Fig. 4b.** CoMFA Electrostatic contour map. The blue colored areas favor electropositive substituents.

this position have lowest activity in the dataset. Likewise, compounds **14**, **15**, **16**, **19** and **21** which doesn't contain bulky substitution at these positions showed low activity level. This information proves that bulky substitution at  $R_4$  and  $R_5$  are highly desirable to increase the activity of the compounds. The yellow contours near the fluoride atom of the  $R_1$  position suggest that bulky substitution at this position could decrease the activity.

The electrostatic contour map of the selected CoMFA model is shown in Fig. 4b. The blue color signifies positive charge is favored and red color signifies that negative charge is favored to increase the activity of the compound. The small blue contour seen near the  $R_3$  substitution indicates that positive substitution in that position could increase the activity. This could validate the fact that compounds **3**, **25** and **26** including the most active compound **27** that contain positive substitution at

this position possess better activity.

#### 4. Conclusions

In this study, we have taken a series of pyrrolopyrimidines as potent antagonist for LIMK2 kinase. Various partial charges were used to develop several models and the final CoMFA model with acceptable statistical values was developed using Pullman as partial charge. The developed model was validated using 1000 runs of bootstrapping and found to be predicable and robust. The analysis of the contour maps of the final CoMFA model highlighted the regions to increase the activity of the compounds. The results of contour maps suggest that bulky positive substitution in  $R_4$  and  $R_5$  positions could enhance the activity. Whereas, Bulky substitution must be strongly avoided in the  $R_1$  position to increase the activity of these compounds Positive substitution in  $R_3$  position can help to enhance the activity of the compounds. The useful information provided by the contour maps could be used to develop a more potent compound of pyrrolopyrimidines based LIMK2 inhibitor.

#### Acknowledgements

This work was supported by the National Research Foundation of Korea grant (MRC, 2015-009070) funded by the Korea government (MSIP)

#### References

- [1] K. Mizuno, I Okano, K. Ohashi, K. Nunoue, K. Kuma, T. Miyata, and T. Nakamura, "Identification of a human cDNA encoding a novel protein kinase with two repeats of the LIM/double zinc finger motif.", *Oncogene*, Vol. 9, pp. 1605-1612, 1994.
- [2] I. Okano, J. Hiraoka, H. Otera, K. Nunoue, K. Ohashi, S. Iwashita, M. Hirai, and K. Mizuno, "Identification and characterization of a novel family of serine/threonine kinases containing two N-terminal LIM motifs", *J. Biol. Chem.*, Vol. 270, pp. 31321-31330, 1995.
- [3] O. Bernard, "Lim kinases, regulators of actin dynamics.", *Int. J. Biochem. Cell B.*, Vol. 39, pp. 1071-1076, 2007.
- [4] K. Ohashi, K. Nagata, M. Maekawa, T. Ishizaki, S. Narumiya, and K. Mizuno, "Rho-associated kinase ROCK activates LIM-kinase 1 by phosphorylation

- at threonine 508 within the activation loop”, *J. Biol. Chem.*, Vol. 275, pp. 3577-3582, 2000.
- [5] T. Amano, K. Tanabe, T. Eto, S. Karumiya, and K. Mizuno, “LIM-kinase 2 induces formation of stress fibres, focal adhesions and membrane blebs, dependent on its activation by Rho-associated kinase-catalysed phosphorylation at threonine -505”, *Biochem J.*, Vol. 354, pp. 149-159, 2001.
- [6] T. Sumi, K. Matsumoto, and T. Nakamura, “Specific activation of LIM kinase 2 via phosphorylation of threonine 505 by ROCK, a Rho-dependent protein kinase”, *J. Biol. Chem.*, Vol. 276, pp. 670-676, 2001.
- [7] F. Manetti, “LIM kinases are attractive targets with many macromolecular partners and only a few small molecule regulators”, *Med. Res. Rev.*, Vol. 32, pp. 968-998, 2012.
- [8] B. A. Harrison, B. A. Harrison, N. A. Whitlock, M. V. Voronkov, Z. Y. Almstead, K.-J. Gu, R. Mabon, M. Gardyan, B. D. Hamman, J. Allen, S. Gopinathan, B. McKnight, M. Crist, Y. Zhang, Y. Liu, L. F. Courtney, B. Key, J. Zhou, N. Patel, P. W. Yates, Q. Liu, A. G. E. Wilson, S. D. Kimball, C. E. Crosson, D. S. Rice, and D. B. Rawlins, “Novel class of LIM-kinase 2 inhibitors for the treatment of ocular hypertension and associated glaucoma”, *J. Med. Chem.*, Vol. 52, pp. 6515-6518, 2009.
- [9] Y.-P. Dai, S. Bongalon, H. Tian, S. D. Parks, V. N. Mutafova-Yambolieva, and L. A. Yamboliev, “Upregulation of profilin, cofilin-2 and LIMK2 in cultured pulmonary artery smooth muscle cells and in pulmonary arteries of monocrotaline-treated rats”, *Vasc. Pharmacol.*, Vol. 44, pp. 275-282, 2006.
- [10] F. Manetti, “HIV-1 proteins join the family of LIM kinase partners. New roads open up for HIV-1 treatment”, *Drug Discov. Today*, Vol.17, pp. 81-88, 2012.
- [11] P. Ross-Macdonald, H. D. Silva, Q. Guo, H. Xiao, C.-Y. Hung, B. Penhallow, J. Markwalder, L. He, R. M. Attar, T.-A. Lin, S. Seitz, C. Tilford, J. Wardwell-Swanson, and D. Jackson, “Identification of a nonkinase target mediating cytotoxicity of novel kinase inhibitors”, *Mol. Cancer Ther.*, Vol. 7, pp. 3490-3498, 2008.
- [12] P. K. Balasubramanian, A. Balupuri, and S. J. Cho, “Ligand-based CoMFA study on pyridylpyrazolopyridine derivatives as PKC $\theta$  kinase inhibitors”, *J. Chosun Natural Sci.*, Vol. 7, pp. 253-259, 2014.
- [13] P. K. Balasubramanian, A. Balupuri, and S. J. Cho, “A CoMFA study of phenoxypyridine-based JNK3 inhibitors using various partial charge schemes”, *J. Chosun Natural Sci.*, Vol. 7, pp. 45-49, 2014.
- [14] P. K. Balasubramanian and S. J. Cho, “HQ SAR analysis on novel series of 1-(4-phenylpiperazin-1-yl)-2-(1H-Pyrazol-1-yl) ethanone derivatives targeting CCR1”, *J. Chosun Natural Sci.*, Vol. 6, pp. 163-169, 2013.
- [15] A. Balupuri and S. J. Cho, “Exploration of the binding mode of indole derivatives as potent HIV-1 inhibitors using molecular docking simulations”, *J. Chosun Natural Sci.*, Vol. 6, pp. 138-142, 2013.
- [16] S. J. Cho, “The importance of halogen bonding: A tutorial”, *J. Chosun Natural Sci.*, Vol. 5, pp. 195-197, 2012.
- [17] S. Boland, A. Bourin, J. Alen, J. Geraets, P. Schrodgers, k. Castermans, N. Kindt, N. Boumans, L. Panitti, J. Vanormelingen, S. Franssen, S. V. D. Velde, and O. Befert, “Design, synthesis and biological characterization of selective LIMK inhibitors”, *Bioorg. Med. Chem. Lett.*, Vol. 25, pp. 4005-4010, 2015.
- [18] SYBYLx2.1, Tripos International, 1699 South Hanley Road, St. Louis, Missouri, 63144, USA.
- [19] R. D. Cramer, D. E. Patterson, and J. D. Bunce, “Comparative molecular field analysis (CoMFA). 1. Effect of shape on binding of steroids to carrier proteins”, *J. Am. Chem. Soc.*, Vol. 110, pp. 5959-5967, 1988.